CHEMISTRY
A European Journal

Supporting Information

Judicious Ligand Design in Ruthenium Polypyridyl CO_2 Reduction Catalysts to Enhance Reactivity by Steric and Electronic Effects

Ben A. Johnson,[a] Hemlata Agarwala,[a] Travis A. White,[a] Edgar Mijangos,[a] Somnath Maji,*[b] and Sascha Ott*[a]

chem_201601612_sm_miscellaneous_information.pdf

Supporting Information

Table S1. Selective experimental (X-ray) and DFT calculated (B3LYP/SDD/6-31G*/ gas phase) bond distances (Å) and bond angles (°) of complexes $(A)^n$ (A = [1]-[5]; *n* = 3+, 2+, +, 0).

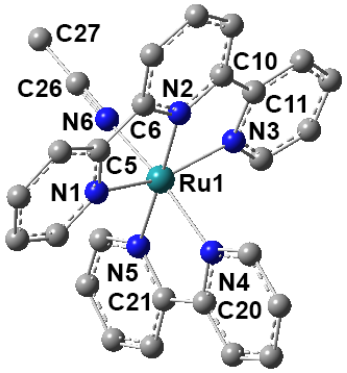

Bond	X-Ray	DFT			
	n = 2+ (*S*=0)	*n* = 2+ (*S*=0)	*n* = 3+ (*S*=1/2)	*n* = 1+ (*S*=1/2)	*n* = 0 (*S*=1)
$[\mathbf{1}]^n$					
Ru(1)-N(1)	2.061	2.119	2.115	2.115	2.105
Ru(1)-N(2)	1.968	2.003	2.051	2.003	2.001
Ru(1)-N(3)	2.071	2.120	2.113	2.114	2.105
Ru(1)-N(4)	2.039	2.091	2.079	2.082	2.084
Ru(1)-N(5)	2.080	2.121	2.089	2.116	2.124
Ru(1)-N(6)	2.037	2.053	2.096	2.028	2.014
C(5)-C(6)	1.465	1.481	1.477	1.454	1.454
C(10)-C(11)	1.477	1.481	1.477	1.453	1.455
C(20)-C(21)	1.476	1.477	1.474	1.475	1.424
N(1)-Ru(1)-N(2)	79.61	78.95	77.38	78.70	78.97
N(1)-Ru(1)-N(3)	159.32	157.88	153.59	157.46	157.89
N(1)-Ru(1)-N(4)	90.17	91.22	88.33	91.27	90.79
N(1)-Ru(1)-N(5)	101.37	101.16	102.44	101.70	101.19
N(1)-Ru(1)-N(6)	88.53	89.95	92.75	89.43	90.13
N(2)-Ru(1)-N(3)	79.72	78.94	77.39	78.76	78.93
N(2)-Ru(1)-N(4)	96.28	97.44	99.43	95.80	95.41
N(2)-Ru(1)-N(5)	174.44	175.07	177.74	173.43	173.88
N(2)-Ru(1)-N(6)	89.13	88.92	85.25	88.81	89.85
N(3)-Ru(1)-N(4)	92.61	91.12	88.21	91.30	90.63
N(3)-Ru(1)-N(5)	99.26	100.83	102.46	100.73	100.71
N(3)-Ru(1)-N(6)	90.63	90.14	92.82	89.79	90.46
N(4)-Ru(1)-N(5)	78.27	77.63	78.31	77.64	78.47
N(4)-Ru(1)-N(6)	174.11	173.64	175.31	175.39	174.73

N(5)-Ru(1)-N(6)	96.36	96.01	97.00	97.75	96.26
C(26)-N(6)-Ru(1)	174.84	178.26	178.88	176.85	178.75
C(27)-C(26)-N(6)	179.42	179.60	179.60	179.87	179.50
[**2**]^n					
Ru(1)-N(1)	2.078	2.121	2.105	2.101	2.102
Ru(1)-N(2)	1.965	2.003	2.042	1.999	2.001
Ru(1)-N(3)	2.079	2.119	2.106	2.125	2.112
Ru(1)-N(4)	2.040	2.091	2.079	2.080	2.085
Ru(1)-N(5)	2.076	2.119	2.098	2.113	2.124
Ru(1)-N(6)	2.038	2.046	2.091	2.030	2.011
C(5)-C(6)	1.473	1.483	1.479	1.448	1.434
C(10)-C(11)	1.485	1.484	1.479	1.477	1.480
C(20)-C(21)	1.477	1.476	1.474	1.460	1.423
N(1)-Ru(1)-N(2)	79.67	78.57	77.29	79.07	79.30
N(1)-Ru(1)-N(3)	158.48	157.30	153.40	157.27	157.55
N(1)-Ru(1)-N(4)	89.84	91.28	88.12	90.83	90.48
N(1)-Ru(1)-N(5)	101.23	101.31	102.45	99.55	101.43
N(1)-Ru(1)-N(6)	87.63	89.92	92.91	89.82	89.42
N(2)-Ru(1)-N(3)	78.82	78.73	77.37	78.19	78.27
N(2)-Ru(1)-N(4)	95.06	97.23	99.48	95.75	95.51
N(2)-Ru(1)-N(5)	173.58	174.87	177.61	173.58	173.88
N(2)-Ru(1)-N(6)	88.82	88.96	85.16	89.41	89.83
N(3)-Ru(1)-N(4)	92.73	91.22	88.18	91.54	90.65
N(3)-Ru(1)-N(5)	100.22	101.27	102.52	103.05	100.77
N(3)-Ru(1)-N(6)	91.23	90.01	92.88	89.83	91.51
N(4)-Ru(1)-N(5)	78.62	77.64	78.13	77.96	78.43
N(4)-Ru(1)-N(6)	174.93	173.81	175.36	174.83	174.55
N(5)-Ru(1)-N(6)	97.56	96.17	97.22	96.88	96.24
C(26)-N(6)-Ru(1)	171.01	178.34	178.91	177.27	178.02
C(27)-C(26)-N(6)	179.70	179.53	179.58	179.68	179.28
cis-[**3**]^n					
Ru(1)-N(1)	2.073	2.119	2.110	2.117	2.104
Ru(1)-N(2)	1.958	1.998	2.042	1.997	1.996
Ru(1)-N(3)	2.063	2.121	2.115	2.113	2.105
Ru(1)-N(4)	2.053	2.084	2.074	2.073	2.076
Ru(1)-N(5)	2.117	2.194	2.163	2.183	2.185
Ru(1)-N(6)	2.047	2.064	2.099	2.040	2.025
C(5)-C(6)	1.469	1.481	1.477	1.456	1.451
C(10)-C(11)	1.483	1.482	1.477	1.453	1.457
C(20)-C(21)	1.448	1.476	1.472	1.473	1.426
N(1)-Ru(1)-N(2)	80.13	79.10	77.72	78.83	79.16
N(1)-Ru(1)-N(3)	160.13	158.17	154.17	157.79	158.18
N(1)-Ru(1)-N(4)	88.36	91.08	88.07	91.17	90.94
N(1)-Ru(1)-N(5)	103.76	101.19	102.09	102.48	101.20
N(1)-Ru(1)-N(6)	86.28	89.39	92.74	88.92	89.19
N(2)-Ru(1)-N(3)	80.00	79.08	77.66	78.96	79.03

N(2)-Ru(1)-N(4)	92.17	95.30	96.96	94.04	93.56
N(2)-Ru(1)-N(5)	169.57	173.01	175.42	171.66	172.11
N(2)-Ru(1)-N(6)	83.95	84.41	81.74	84.51	84.93
N(3)-Ru(1)-N(4)	92.37	90.43	87.24	90.65	90.07
N(3)-Ru(1)-N(5)	95.82	100.41	101.82	99.53	100.35
N(3)-Ru(1)-N(6)	91.66	88.99	91.38	88.71	89.23
N(4)-Ru(1)-N(5)	78.38	77.73	78.47	77.74	78.56
N(4)-Ru(1)-N(6)	173.85	179.39	178.28	178.50	178.43
N(5)-Ru(1)-N(6)	105.83	102.56	102.82	103.69	102.94
C(26)-N(6)-Ru(1)	167.23	172.59	174.48	170.91	171.16
C(27)-C(26)-N(6)	179.36	178.17	178.39	178.99	178.34
trans-[**3**]^n					
Ru(1)-N(1)	2.073	2.121	2.111	2.114	2.104
Ru(1)-N(2)	1.958	2.009	2.051	2.007	2.006
Ru(1)-N(3)	2.063	2.120	2.111	2.115	2.107
Ru(1)-N(4)	2.063	2.170	2.149	2.165	2.154
Ru(1)-N(5)	2.115	2.109	2.090	2.097	2.113
Ru(1)-N(6)	2.047	2.045	2.093	2.018	2.005
C(5)-C(6)	1.469	1.481	1.477	1.455	1.449
C(10)-C(11)	1.483	1.481	1.477	1.455	1.463
C(20)-C(21)	1.442	1.476	1.472	1.472	1.424
N(1)-Ru(1)-N(2)	80.13	78.84	77.34	78.75	79.11
N(1)-Ru(1)-N(3)	160.13	157.60	153.04	157.42	157.81
N(1)-Ru(1)-N(4)	88.12	92.31	88.95	94.08	93.67
N(1)-Ru(1)-N(5)	98.73	101.22	102.83	102.47	101.76
N(1)-Ru(1)-N(6)	86.28	89.58	92.71	88.75	89.13
N(2)-Ru(1)-N(3)	80.00	78.82	77.35	78.68	78.73
N(2)-Ru(1)-N(4)	109.80	104.65	105.63	102.73	102.45
N(2)-Ru(1)-N(5)	171.25	177.51	175.89	178.62	178.62
N(2)-Ru(1)-N(6)	83.95	84.04	81.49	84.56	85.16
N(3)-Ru(1)-N(4)	98.58	91.74	89.02	90.44	89.96
N(3)-Ru(1)-N(5)	100.91	101.16	103.08	100.11	100.42
N(3)-Ru(1)-N(6)	91.66	89.71	92.61	89.55	90.15
N(4)-Ru(1)-N(5)	78.76	77.84	78.48	77.86	78.60
N(4)-Ru(1)-N(6)	167.03	171.31	172.88	172.56	172.26
N(5)-Ru(1)-N(6)	87.32	93.48	94.40	94.81	93.77
C(26)-N(6)-Ru(1)	167.23	177.34	178.52	175.97	177.64
C(27)-C(26)-N(6)	179.36	179.18	179.34	179.85	179.21
cis-[**4**]^n					
Ru(1)-N(1)	-	2.121	2.103	2.115	2.104
Ru(1)-N(2)	-	1.998	2.033	1.992	1.996
Ru(1)-N(3)	-	2.119	2.104	2.115	2.111
Ru(1)-N(4)	-	2.083	2.075	2.071	2.076
Ru(1)-N(5)	-	2.193	2.175	2.175	2.182
Ru(1)-N(6)	-	2.057	2.096	2.039	2.021
C(5)-C(6)	-	1.484	1.479	1.454	1.433

C(10)-C(11)	-	1.485	1.480	1.470	1.480
C(20)-C(21)	-	1.476	1.473	1.463	1.425
N(1)-Ru(1)-N(2)	-	78.74	77.64	78.74	79.36
N(1)-Ru(1)-N(3)	-	157.63	154.09	157.42	157.82
N(1)-Ru(1)-N(4)	-	90.71	87.65	90.63	90.99
N(1)-Ru(1)-N(5)	-	100.97	101.80	103.83	102.75
N(1)-Ru(1)-N(6)	-	89.12	92.22	89.21	88.95
N(2)-Ru(1)-N(3)	-	78.89	77.69	78.68	78.48
N(2)-Ru(1)-N(4)	-	95.02	96.79	94.19	93.55
N(2)-Ru(1)-N(5)	-	172.75	175.06	171.64	171.74
N(2)-Ru(1)-N(6)	-	84.44	81.72	85.13	85.36
N(3)-Ru(1)-N(4)	-	90.79	87.51	90.46	89.46
N(3)-Ru(1)-N(5)	-	101.16	102.09	98.45	99.07
N(3)-Ru(1)-N(6)	-	89.16	91.96	89.43	90.18
N(4)-Ru(1)-N(5)	-	77.73	78.27	77.91	78.49
N(4)-Ru(1)-N(6)	-	179.46	178.50	179.32	178.90
N(5)-Ru(1)-N(6)	-	102.80	103.22	102.77	102.59
C(26)-N(6)-Ru(1)	-	172.56	174.39	171.72	171.52
C(27)-C(26)-N(6)	-	178.09	178.39	178.75	178.28
trans-[**4**]^n					
Ru(1)-N(1)	-	2.122	2.102	2.109	2.102
Ru(1)-N(2)	-	2.010	2.044	2.003	2.007
Ru(1)-N(3)	-	2.121	2.103	2.120	2.114
Ru(1)-N(4)	-	2.170	2.149	2.159	2.154
Ru(1)-N(5)	-	2.108	2.098	2.096	2.113
Ru(1)-N(6)	-	2.036	2.088	2.019	2.002
C(5)-C(6)	-	1.484	1.479	1.454	1.433
C(10)-C(11)	-	1.484	1.479	1.473	1.482
C(20)-C(21)	-	1.476	1.472	1.460	1.424
N(1)-Ru(1)-N(2)	-	78.45	77.25	78.72	79.25
N(1)-Ru(1)-N(3)	-	157.04	152.89	157.05	157.45
N(1)-Ru(1)-N(4)	-	91.43	88.91	94.07	93.98
N(1)-Ru(1)-N(5)	-	101.22	102.84	103.33	102.68
N(1)-Ru(1)-N(6)	-	89.53	92.77	88.59	88.41
N(2)-Ru(1)-N(3)	-	78.63	77.33	78.35	78.24
N(2)-Ru(1)-N(4)	-	104.31	105.74	103.05	102.58
N(2)-Ru(1)-N(5)	-	177.87	175.95	177.67	177.77
N(2)-Ru(1)-N(6)	-	84.23	81.43	84.81	85.19
N(3)-Ru(1)-N(4)	-	92.91	89.04	90.04	89.51
N(3)-Ru(1)-N(5)	-	101.73	103.19	99.61	99.86
N(3)-Ru(1)-N(6)	-	89.50	92.61	90.41	91.12
N(4)-Ru(1)-N(5)	-	77.78	78.31	78.01	78.50
N(4)-Ru(1)-N(6)	-	171.43	172.83	172.04	172.17
N(5)-Ru(1)-N(6)	-	93.67	94.52	94.09	93.71
C(26)-N(6)-Ru(1)	-	177.36	178.52	177.00	177.56
C(27)-C(26)-N(6)	-	179.10	179.31	179.54	179.10

[**5**]^n					
Ru(1)-N(1)		2.117	2.105	2.115	2.104
Ru(1)-N(2)	-	2.003	2.047	2.000	2.002
Ru(1)-N(3)	-	2.129	2.124	2.121	2.114
Ru(1)-N(4)	-	2.153	2.137	2.146	2.139
Ru(1)-N(5)	-	2.165	2.134	2.149	2.162
Ru(1)-N(6)	-	2.052	2.096	2.030	2.014
C(5)-C(6)	-	1.481	1.477	1.456	1.439
C(10)-C(11)	-	1.481	1.476	1.455	1.468
C(20)-C(21)	-	1.480	1.475	1.474	1.429
N(1)-Ru(1)-N(2)	-	79.09	77.59	78.90	79.42
N(1)-Ru(1)-N(3)	-	157.90	153.49	157.73	158.08
N(1)-Ru(1)-N(4)	-	96.02	91.69	96.15	95.88
N(1)-Ru(1)-N(5)	-	102.16	102.00	103.54	102.79
N(1)-Ru(1)-N(6)	-	90.45	94.67	89.11	88.96
N(2)-Ru(1)-N(3)	-	78.84	77.28	78.83	78.66
N(2)-Ru(1)-N(4)	-	101.39	103.31	100.13	99.70
N(2)-Ru(1)-N(5)	-	178.57	178.02	176.98	177.15
N(2)-Ru(1)-N(6)	-	82.24	80.14	82.22	82.83
N(3)-Ru(1)-N(4)	-	87.34	85.98	87.95	87.57
N(3)-Ru(1)-N(5)	-	99.89	103.40	98.72	99.11
N(3)-Ru(1)-N(6)	-	87.59	89.23	87.69	88.56
N(4)-Ru(1)-N(5)	-	77.83	78.61	77.94	78.35
N(4)-Ru(1)-N(6)	-	173.07	173.30	174.56	174.87
N(5)-Ru(1)-N(6)	-	98.41	97.99	99.51	98.94
C(26)-N(6)-Ru(1)	-	172.94	174.33	171.12	171.62
C(27)-C(26)-N(6)	-	178.04	178.56	178.78	178.20

Table S2. Selected DFT calculated (B3LYP/SDD/6-31G*/gas phase) bond distances and angles for mono- and bi-reduced Ru-CH_3CN and Ru-CO_2 complexes A^{n+} (A = [1]-[5]; *n* = 1, 0)

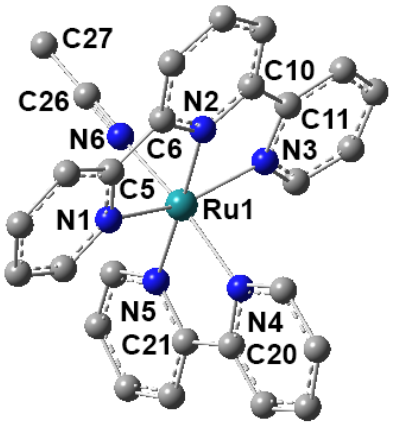

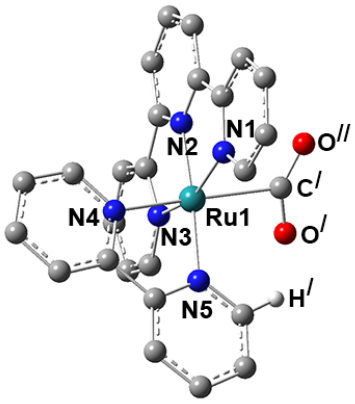

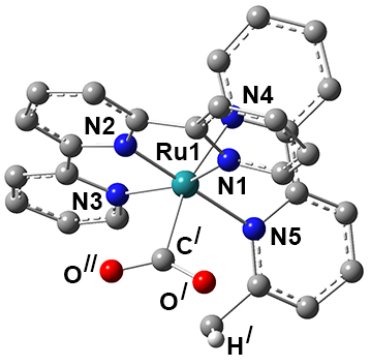

Bond	*n* = 1+		*n* = 0	
	Ru-CH_3CN complex (*S*=1/2)	Ru-CO_2 complex (*S*=1/2)	Ru-CH_3CN complex (*S*=1)	Ru-CO_2 complex (*S*=0)
[**1**]^n				
Ru(1)-N(1)	2.115	2.103	2.105	2.079
Ru(1)-N(2)	2.003	1.982	2.001	1.945
Ru(1)-N(3)	2.114	2.109	2.105	2.084
Ru(1)-N(4)	2.082	2.163	2.084	2.236
Ru(1)-N(5)	2.116	2.141	2.124	2.184
Ru(1)-N(6)	2.028	-	2.014	-
Ru(1)-C$^/$	-	2.318	-	2.176
C$^/$-O$^/$	-	1.227	-	1.251
C$^/$-O$^{//}$	-	1.209	-	1.242
H$^/$····O$^/$	-	2.172	-	1.926
O$^/$-C$^/$-O$^{//}$	-	144.11	-	131.65
[**2**]^n				
Ru(1)-N(1)	2.101	2.106	2.102	2.078
Ru(1)-N(2)	1.999	1.985	2.001	1.948
Ru(1)-N(3)	2.125	2.111	2.112	2.088
Ru(1)-N(4)	2.080	2.169	2.085	2.250
Ru(1)-N(5)	2.113	2.137	2.124	2.177
Ru(1)-N(6)	2.030	-	2.011	-
Ru(1)-C$^/$	-	2.278	-	2.161
C$^/$-O$^/$	-	1.233	-	1.254
C$^/$-O$^{//}$	-	1.211	-	1.244
H$^/$····O$^/$	-	2.163	-	1.908
O$^/$-C$^/$-O$^{//}$	-	142.47	-	130.86
cis-[**3**]^n				
Ru(1)-N(1)	2.117	2.097	2.104	2.102
Ru(1)-N(2)	1.997	1.974	1.996	1.943

Ru(1)-N(3)	2.113	2.098	2.105	2.078
Ru(1)-N(4)	2.073	2.096	2.076	2.192
Ru(1)-N(5)	2.183	2.127	2.185	2.229
Ru(1)-N(6)	2.040	-	2.025	-
Ru(1)-C$^{/}$	-	3.969	-	2.196
C$^{/}$-O$^{/}$	-	1.170	-	1.240
C$^{/}$-O$^{//}$	-	1.169	-	1.240
H$^{/}$····O$^{/}$	-	-	-	2.261
O$^{/}$-C$^{/}$-O$^{//}$	-	179.84	-	134.19
trans-[**3**]^{n}				
Ru(1)-N(1)	2.114	2.106	2.104	2.076
Ru(1)-N(2)	2.007	1.987	2.006	1.949
Ru(1)-N(3)	2.115	2.119	2.107	2.093
Ru(1)-N(4)	2.165	2.283	2.154	2.375
Ru(1)-N(5)	2.097	2.136	2.113	2.172
Ru(1)-N(6)	2.018	-	2.005	-
Ru(1)-C$^{/}$	-	2.288	-	2.163
C$^{/}$-O$^{/}$	-	1.230	-	1.252
C$^{/}$-O$^{//}$	-	1.207	-	1.241
H$^{/}$····O$^{/}$	-	2.127	-	1.896
O$^{/}$-C$^{/}$-O$^{//}$	-	143.73	-	131.55
cis-[**4**]^{n}				
Ru(1)-N(1)	2.115	2.098	2.104	2.077
Ru(1)-N(2)	1.992	1.974	1.996	1.946
Ru(1)-N(3)	2.115	2.100	2.111	2.105
Ru(1)-N(4)	2.071	2.106	2.076	2.208
Ru(1)-N(5)	2.175	2.126	2.182	2.225
Ru(1)-N(6)	2.039	-	2.021	-
Ru(1)-C$^{/}$	-	3.935	-	2.176
C$^{/}$-O$^{/}$	-	1.169	-	1.243
C$^{/}$-O$^{//}$	-	1.170	-	1.242
H$^{/}$····O$^{/}$	-	-	-	2.241
O$^{/}$-C$^{/}$-O$^{//}$	-	179.59	-	133.36
trans-[**4**]^{n}				
Ru(1)-N(1)	2.109	2.124	2.102	2.081
Ru(1)-N(2)	2.003	1.991	2.007	1.950
Ru(1)-N(3)	2.120	2.110	2.114	2.086
Ru(1)-N(4)	2.159	2.304	2.154	2.387
Ru(1)-N(5)	2.096	2.136	2.113	2.173
Ru(1)-N(6)	2.019	-	2.002	-
Ru(1)-C$^{/}$	-	2.229	-	2.141
C$^{/}$-O$^{/}$	-	1.237	-	1.252
C$^{/}$-O$^{//}$	-	1.210	-	1.244
H$^{/}$····O$^{/}$	-	2.127	-	1.974
O$^{/}$-C$^{/}$-O$^{//}$	-	141.60	-	131.21
[**5**]^{n}				

Ru(1)-N(1)	2.115	2.098	2.104	2.105
Ru(1)-N(2)	2.000	1.971	2.002	1.943
Ru(1)-N(3)	2.121	2.098	2.114	2.075
Ru(1)-N(4)	2.146	2.168	2.139	2.307
Ru(1)-N(5)	2.149	2.120	2.162	2.229
Ru(1)-N(6)	2.030	-	2.014	-
Ru(1)-C$^{/}$	-	4.128	-	2.167
C$^{/}$-O$^{/}$	-	1.170	-	1.243
C$^{/}$-O$^{//}$	-	1.169	-	1.240
H$^{/}$····O$^{/}$	-	-	-	2.275
O$^{/}$-C$^{/}$-O$^{//}$	-	179.71	-	133.58

Table S3. Electronic Absorption Data[a]

Complex	λ_{abs} (nm) (ε x 10^{-4} / $M^{-1}cm^{-1}$)
[**1**]$^{2+}$	280 (4.42), 307 (4.23), 455 (1.12)
[**2**]$^{2+}$	285 (4.45), 305 (4.61), 455 (1.31)
[**3**]$^{2+}$	300 (3.47), 450 (0.742)
trans-[**4**]$^{2+}$	305 (5.18), 455 (1.18)
[**5**]$^{2+}$	280 (2.33), 305 (4.21), 455 (0.798)

[a]Measured in 50 μM CH_3CN solution at room temperature.

Table S4. Crystallographic data for compound [1]$(PF_6)_2.H_2O$

Chemical formula	$C_{29}H_{26}N_6Ru·2(F_6P)·H_2O$
M_r	867.58
Crystal system, space group	Monoclinic, $P2_1/c$
Temperature (K)	100
a, b, c (Å)	8.6875 (7), 10.5832 (8), 37.995 (3)
β (°)	94.273 (3)
V (Å^3)	3483.6 (5)
Z	4
Radiation type	Mo $K\alpha$
μ (mm^{-1})	0.64
Crystal size (mm)	0.06 × 0.05 × 0.04
Data collection	
Diffractometer	Bruker *APEX*-II CCD
Absorption correction	Multi-scan *SADABS* (Siemens, 1996)
T_{min}, T_{max}	0.672, 0.745
No. of measured, independent and observed [$I > 2\sigma(I)$] reflections	21074, 5598, 4150
R_{int}	0.063
(sin $\theta/\lambda)_{max}$ (Å^{-1})	0.578
Refinement	
$R[F^2 > 2\sigma(F^2)]$, $wR(F^2)$, S	0.049, 0.109, 1.02
No. of reflections	5598
No. of parameters	469
No. of restraints	2
H-atom treatment	H atoms treated by a mixture of independent and constrained refinement
$\Delta\rho_{max}$, $\Delta\rho_{min}$ (e Å^{-3})	0.59, −0.75

Table S5. Crystallographic data for compound [2]$(PF_6)_2.3CH_3CN$

Chemical formula	$C_{41}H_{50}N_6Ru\cdot 2(F_6P)\cdot 3(C_2H_3N)$
M_r	1141.04
Crystal system, space group	Triclinic, *P*1
Temperature (K)	100
a, *b*, *c* (Å)	12.5027 (10), 12.8376 (10), 17.5745 (14)
α, β, γ (°)	83.030 (4), 72.186 (4), 75.051 (4)
V (Å^3)	2591.9 (4)
Z	2
Radiation type	Mo *K*α
μ (mm^{-1})	0.45
Crystal size (mm)	0.16 × 0.12 × 0.1
Data collection	
Diffractometer	Bruker *APEX*-II CCD
Absorption correction	Multi-scan *SADABS* (Siemens, 1996)
T_{min}, T_{max}	0.663, 0.745
No. of measured, independent and observed [$I > 2\sigma(I)$] reflections	40484, 11288, 9474
R_{int}	0.069
$(\sin \theta/\lambda)_{max}$ (Å^{-1})	0.640
Refinement	
$R[F^2 > 2\sigma(F^2)]$, $wR(F^2)$, *S*	0.047, 0.127, 1.04
No. of reflections	11288
No. of parameters	704
No. of restraints	327
H-atom treatment	H-atom parameters not refined
$\Delta\rho_{max}$, $\Delta\rho_{min}$ (e Å^{-3})	1.37, −0.8

Table S6. Crystallographic data for compound [3](PF$_6$)$_2$.CH$_3$CN (*cis* and *trans*)

Chemical formula	$C_{28}H_{24}N_6Ru\cdot 2(F_6P)\cdot C_2H_3N$
M_r	876.59
Crystal system, space group	Monoclinic, $P2_1/c$
Temperature (K)	100
a, b, c (Å)	19.9204 (6), 10.6076 (3), 16.4054 (5)
β (°)	103.024 (2)
V (Å^3)	3377.41 (18)
Z	4
Radiation type	Mo $K\alpha$
μ (mm^{-1})	0.66
Crystal size (mm)	0.3 × 0.08 × 0.02
Data collection	
Diffractometer	Bruker *APEX*-II CCD
Absorption correction	Multi-scan *SADABS* (Siemens, 1996)
T_{min}, T_{max}	0.653, 0.745
No. of measured, independent and observed [$I > 2\sigma(I)$] reflections	44242, 6570, 5695
R_{int}	0.040
$(\sin\theta/\lambda)_{max}$ (Å^{-1})	0.616
Refinement	
$R[F^2 > 2\sigma(F^2)]$, $wR(F^2)$, S	0.048, 0.097, 1.21
No. of reflections	6570
No. of parameters	591
No. of restraints	571
H-atom treatment	H-atom parameters not refined
	$w = 1/[\sigma^2(F_o^2) + 12.5785P]$ where $P = (F_o^2 + 2F_c^2)/3$
$\Delta\rho_{max}$, $\Delta\rho_{min}$ (e Å^{-3})	0.80, −0.88

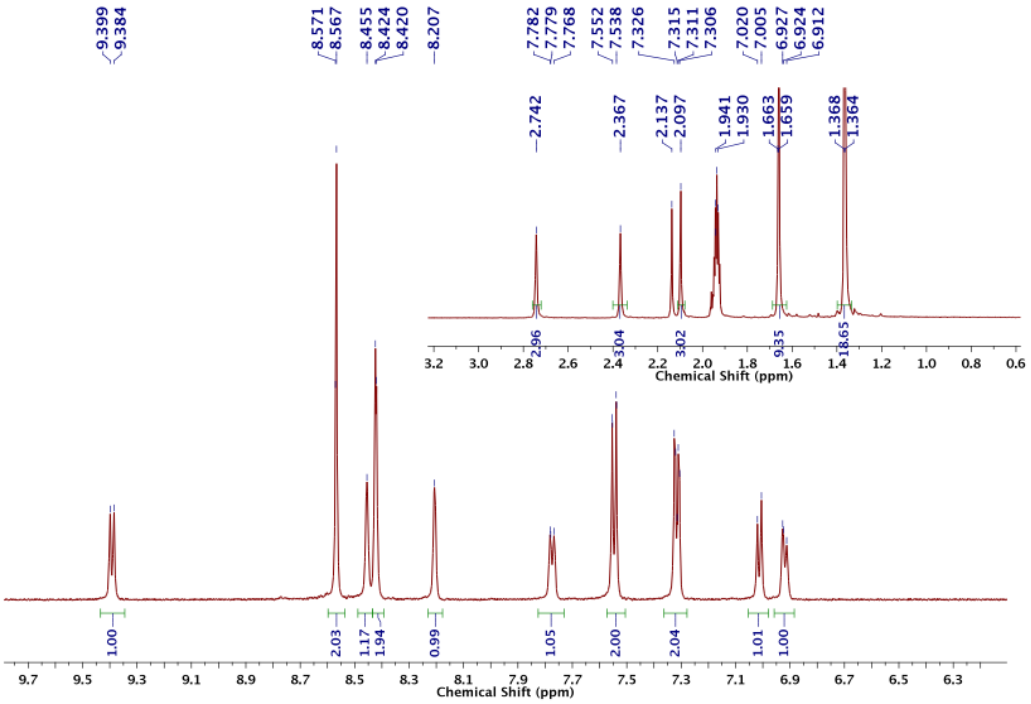

Figure S1a. ^{1}H-NMR spectrum (400 MHz, CD_3CN) of $[\mathbf{2}]^{2+}$ at 298 K.

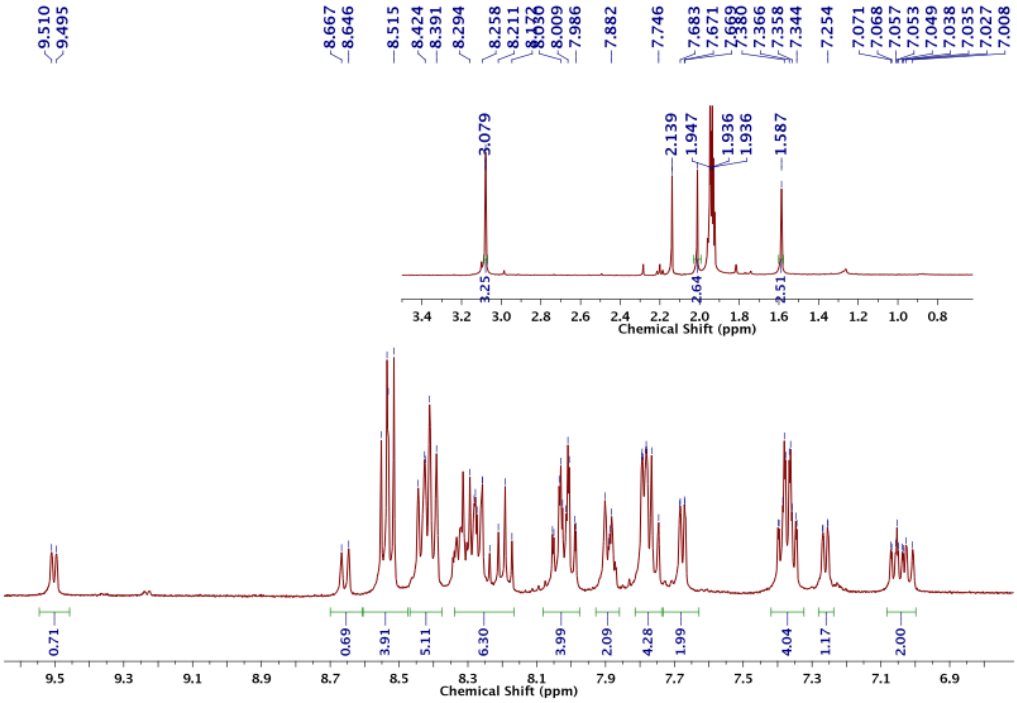

Figure S1b. ^{1}H-NMR spectrum (400 MHz, CD_3CN) of $[\mathbf{3}]^{2+}$ at 298 K.

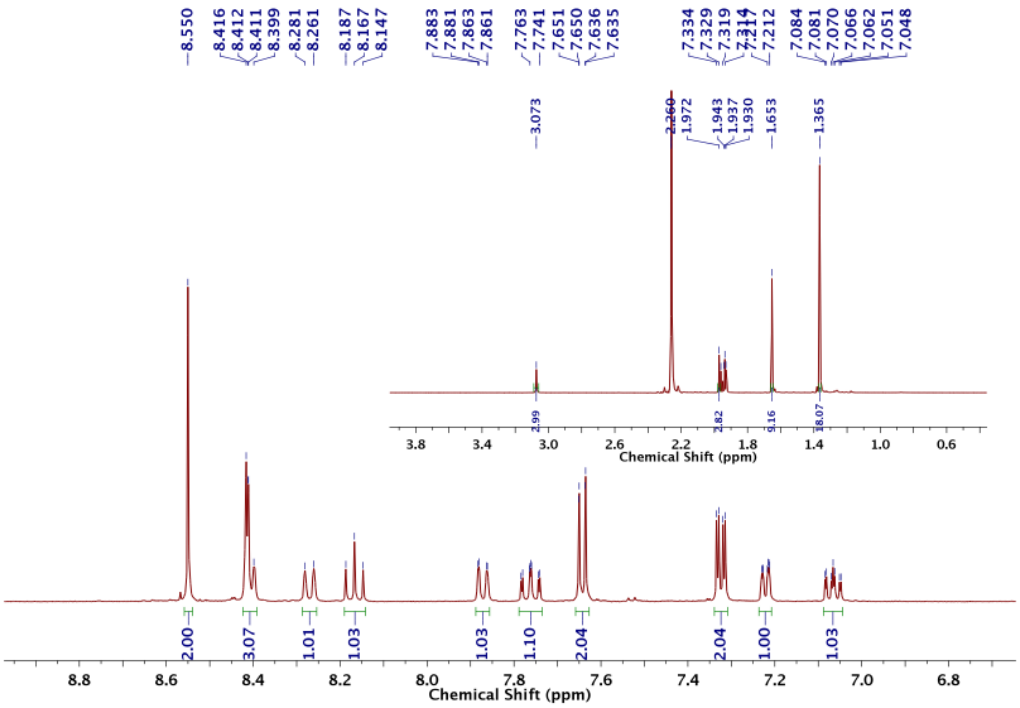

Figure S1c. ^{1}H-NMR spectrum (400 MHz, CD_3CN) of *trans*-[**4**]$^{2+}$ at 298 K.

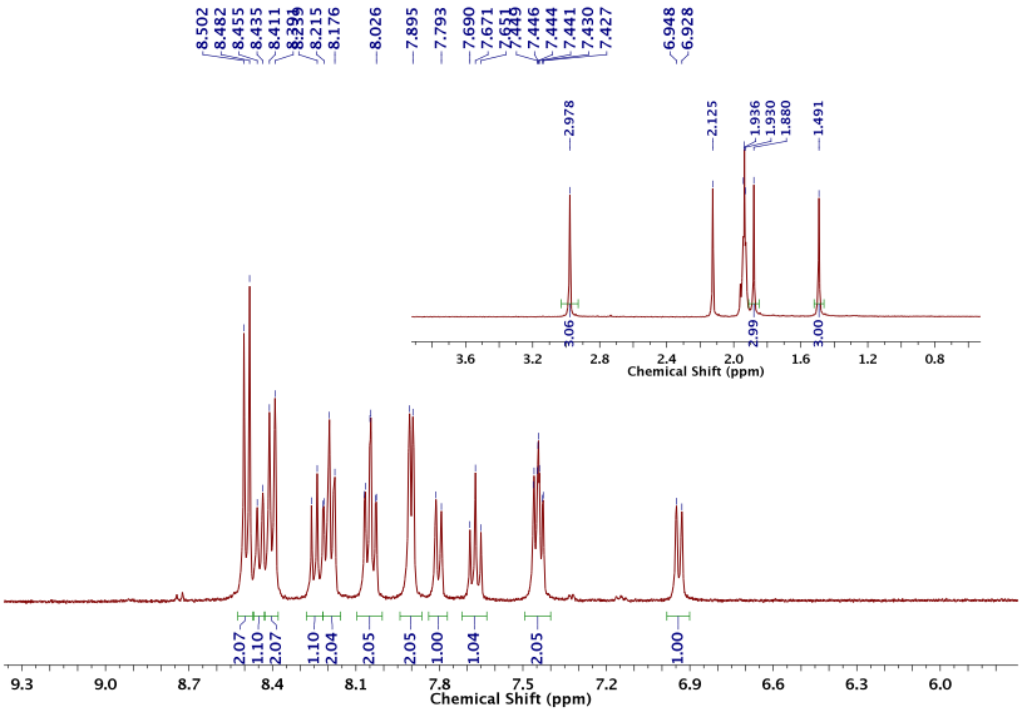

Figure S1d. ^{1}H-NMR spectrum (400 MHz, CD_3CN) of [**5**]$^{2+}$ at 298 K.

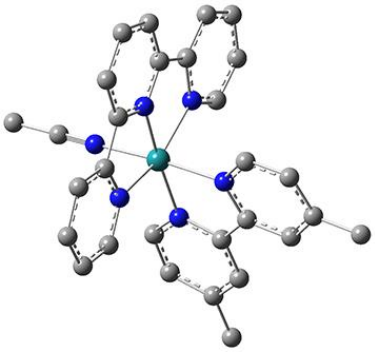

[**1**]$^{2+}$ (*S*=0)

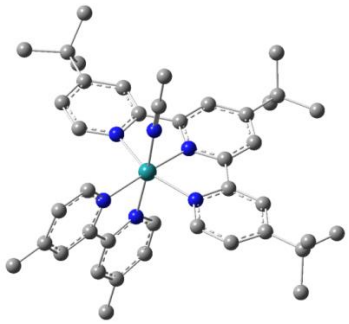

[**2**]$^{2+}$ (*S*=0)

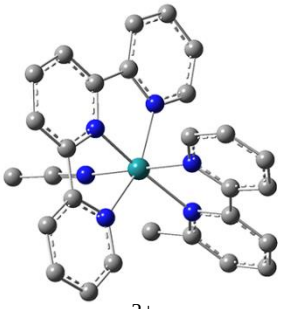

cis-[**3**]$^{2+}$ (*S*=0)

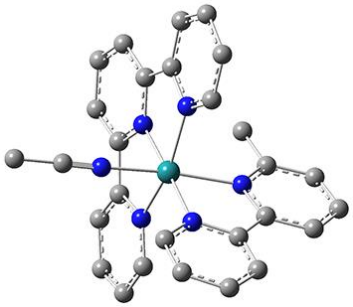

trans-[**3**]$^{2+}$ (*S*=0)

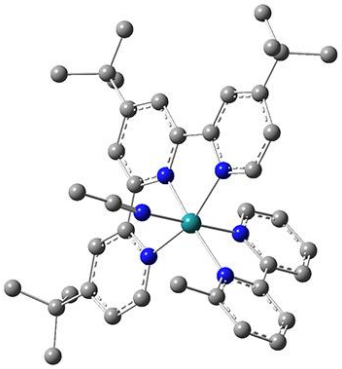

cis-[**4**]$^{2+}$ (*S*=0)

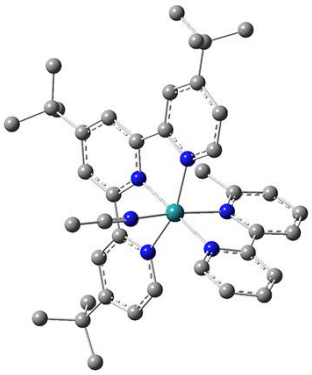

trans-[**4**]$^{2+}$ (*S*=0)

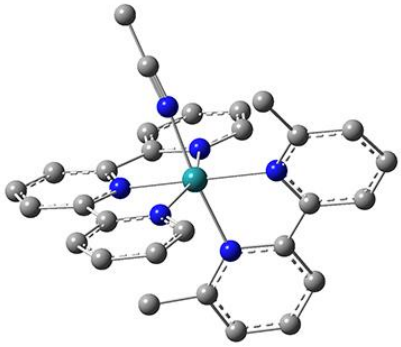

[**5**]$^{2+}$ (*S*=0)

Figure S2. DFT (B3LYP/6-31G*/SDD/gas phase) optimized structures of the complexes.

Compound	n = 3 (S = 1/2)	n = 1 (S = 1/2)	n = 0 (S = 1)
[**1**]^n	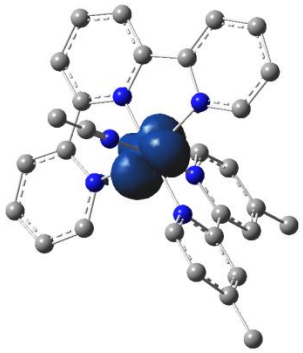	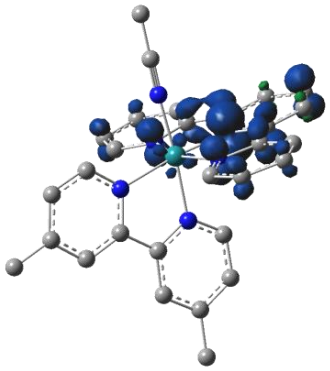	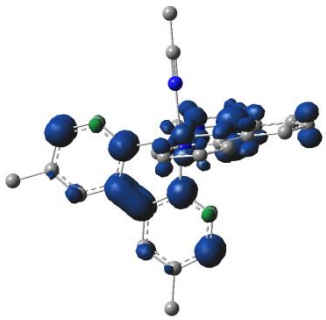
[**2**]^n	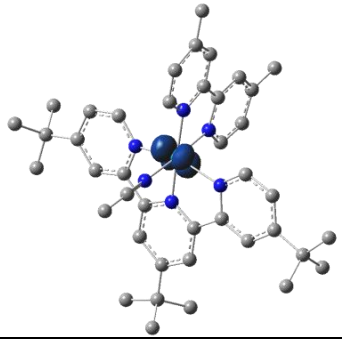	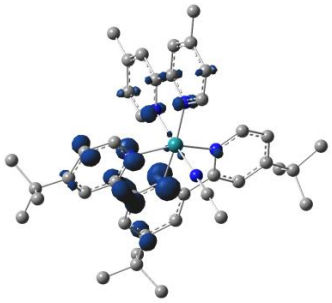	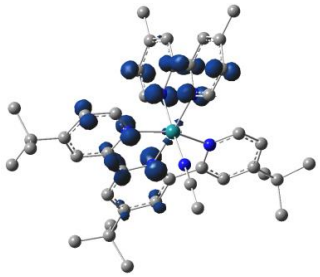
cis-[**3**]^n	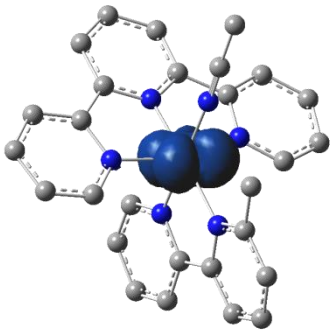	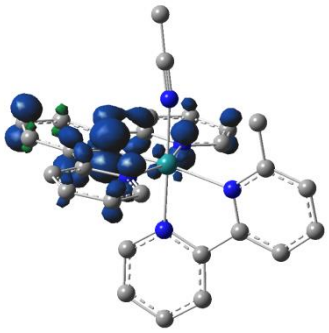	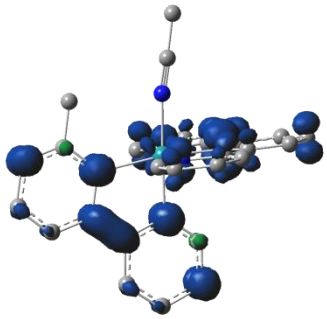
trans-[**3**]^n	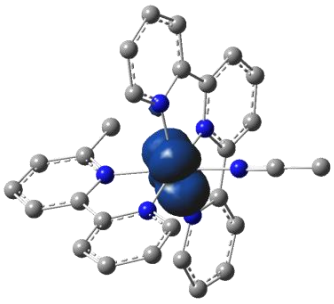	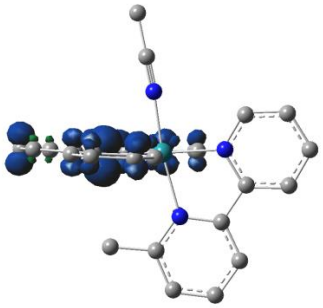	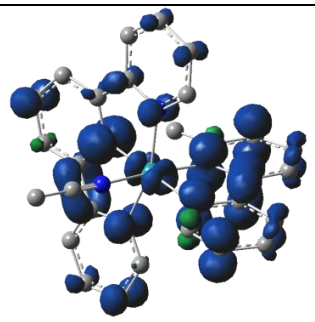
cis-[**4**]^n	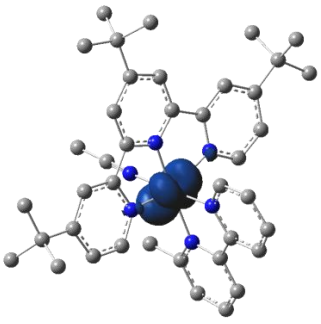	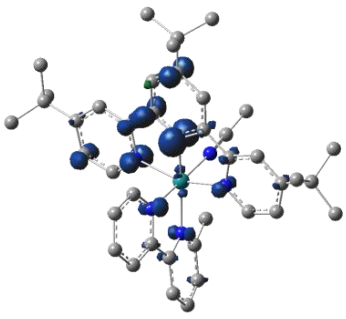	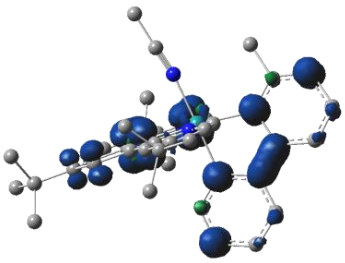

trans-[**4**]^n	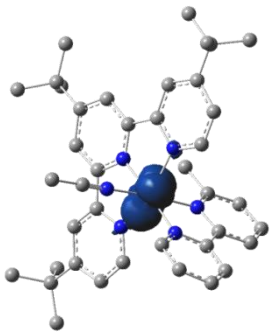	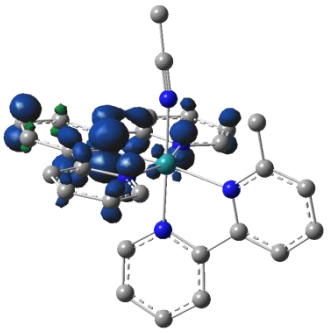	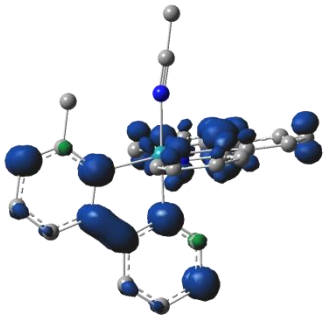
[**5**]^n	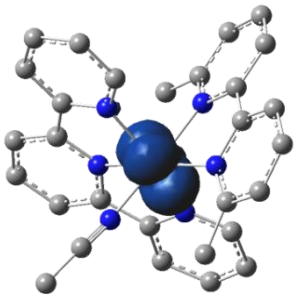	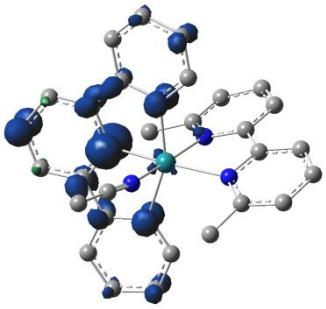	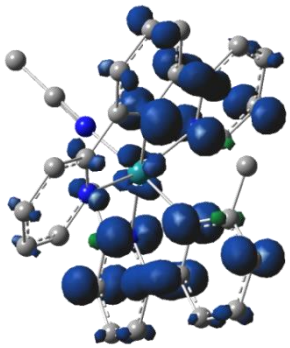

Figure S3. DFT calculated Mulliken spin density representations (B3LYP/6-31G*/SDD/ gas phase) of complexes **A**^{n} (**A** = [**1**]-[**5**] n = 3+, 1+, 0)

Compound	n = 1 (S=1/2)	n = 0 (S=0)
[**1**]$^{n+}$	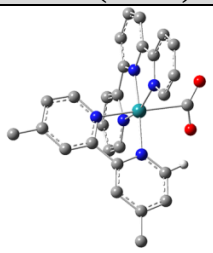	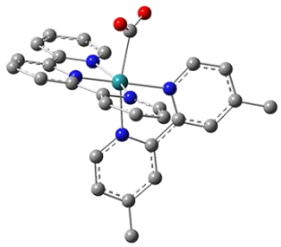
[**2**]$^{n+}$	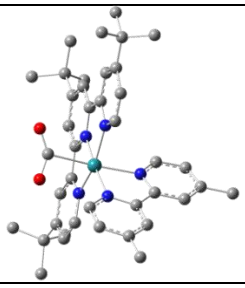	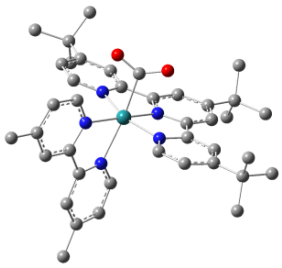
cis-[**3**]$^{n+}$	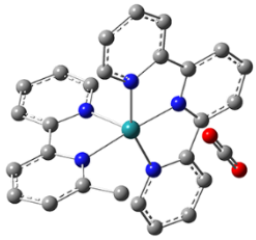	
trans-[**3**]$^{n+}$	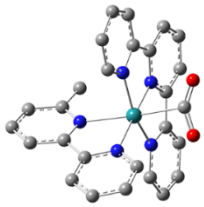	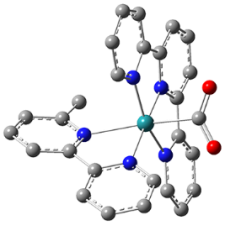
cis-[**4**]$^{n+}$	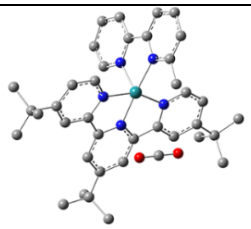	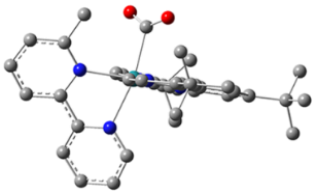
trans-[**4**]$^{n+}$		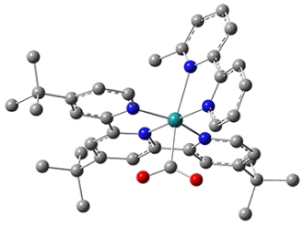
[**5**]$^{n+}$	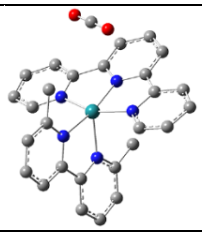	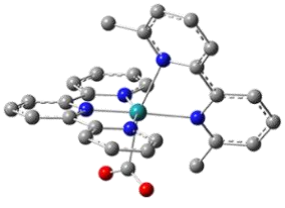

Figure S4. DFT optimized (B3LYP/SDD/6-31G*/gas phase) structures of the mono- and bi-reduced Ru-CO_2 complexes

color gradient : Negative  **Positive**

Compound	Ru-CH_3CN complex		Ru-CO_2 complex	
	spin state (*S*)	ESP mapped over total electron density	spin state (*S*)	ESP mapped over total electron density
$[\mathbf{1}]^+$	1/2	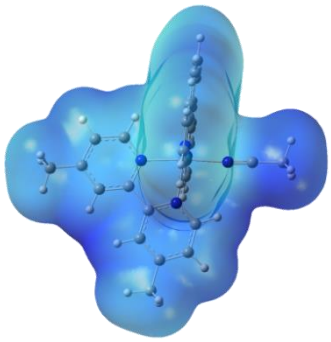	1/2	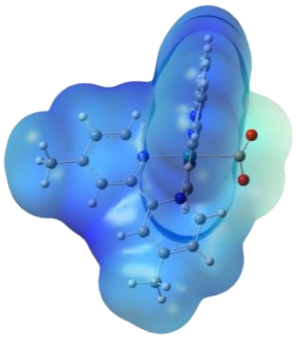
$[\mathbf{1}]^0$	1	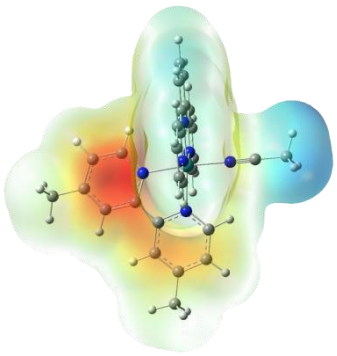	0	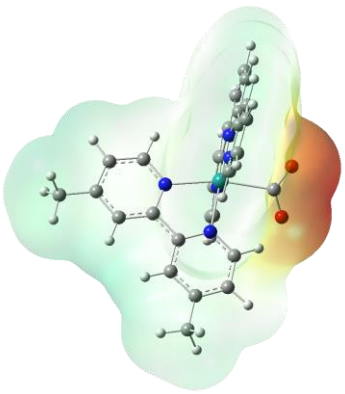
$[\mathbf{2}]^+$	1/2	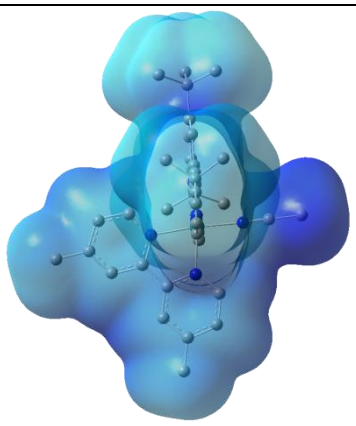	1/2	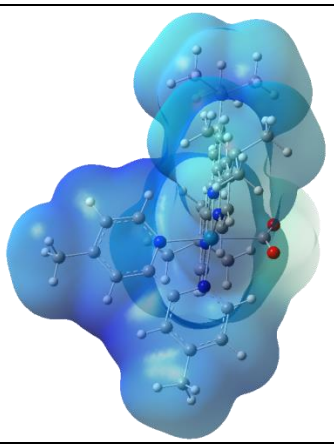
$[\mathbf{2}]^0$	1	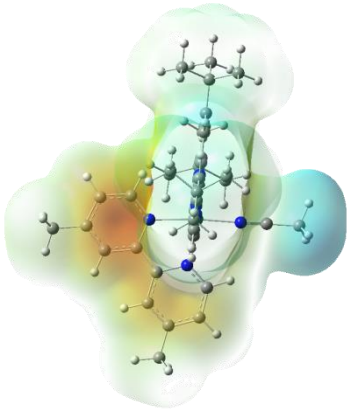	0	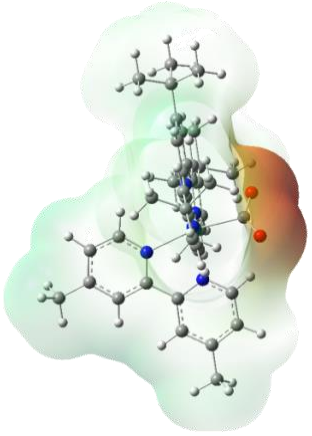

cis-[**3**]$^{+}$	1/2	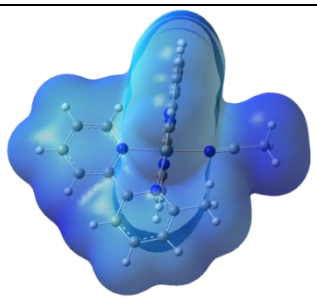	1/2	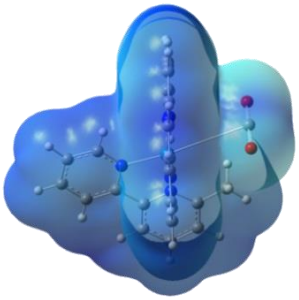
cis-[**3**]^{0}	1	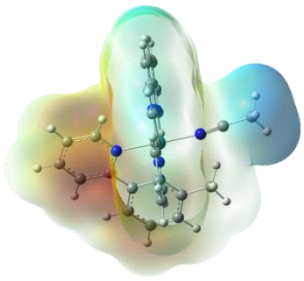	0	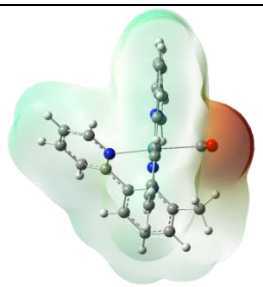
trans-[**3**]$^{+}$	1/2	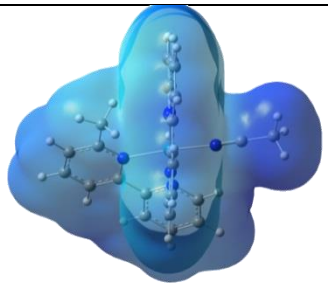	1/2	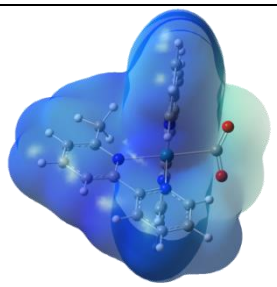
trans-[**3**]^{0}	1	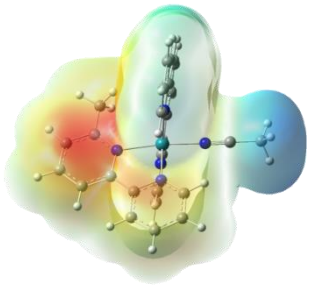	0	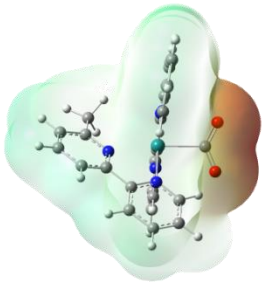
cis-[**4**]$^{+}$	1/2	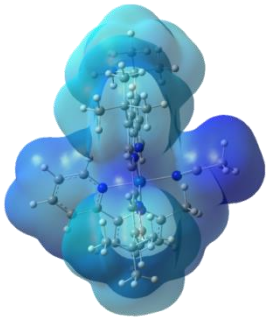	1/2	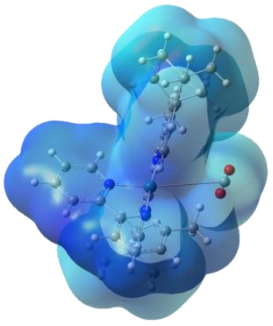
cis-[**4**]^{0}	1	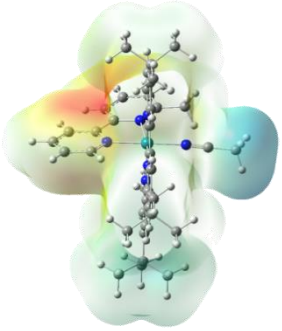	0	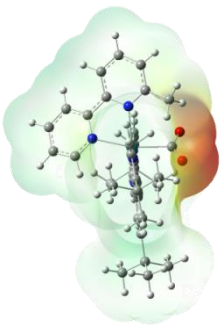

trans-[**4**]$^{+}$	1/2	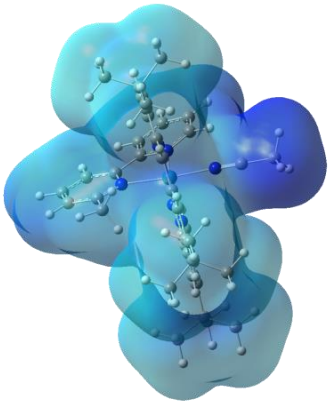	1/2	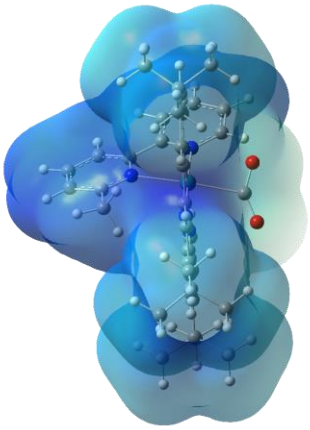
trans-[**4**]^{0}	1	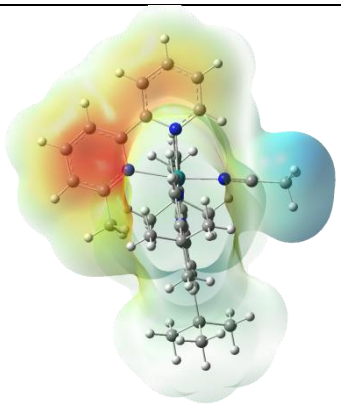	0	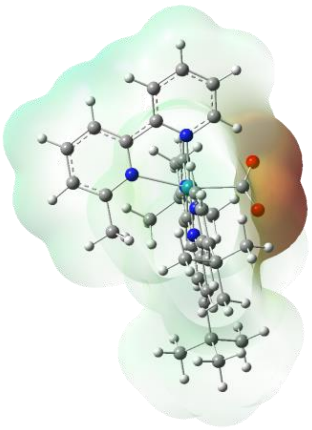
[**5**]$^{+}$	1/2	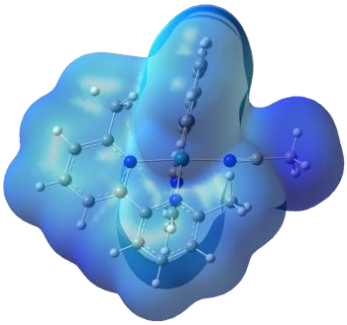	1/2	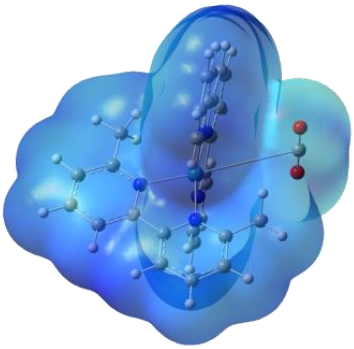
[**5**]^{0}	1	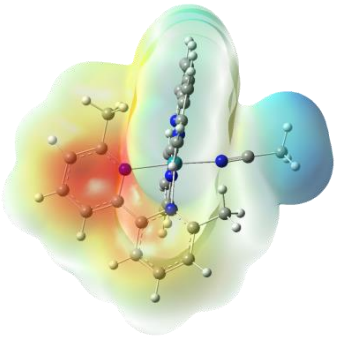	0	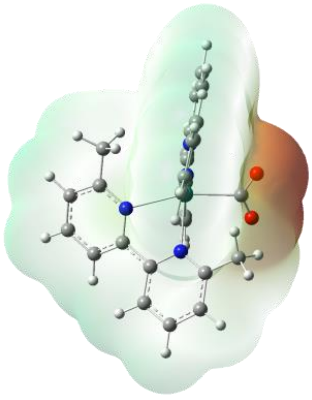

Figure S5. The electrostatic potential mapped on the surface of molecular electron density (isodensity, 0.0004 e^{-3}) of mono-reduced (**A**$^{+}$) and bi-reduced (**A**) (**A** = [**1**]-[**5**]) Ru-CH_3CN and Ru-CO_2 complexes.

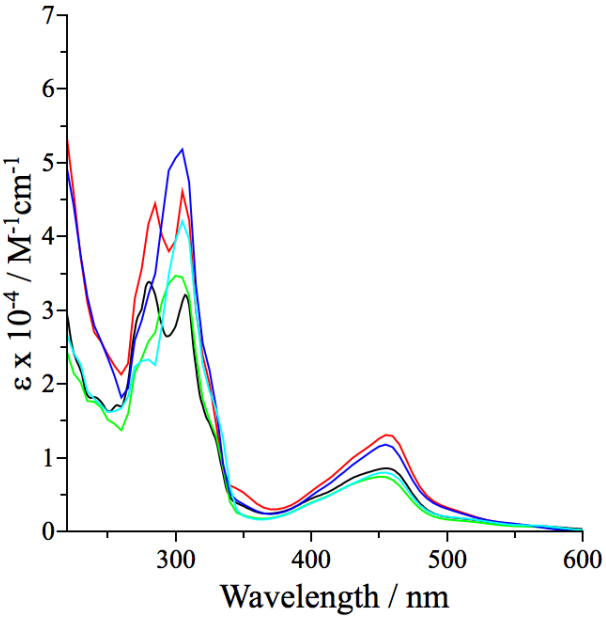

Figure S7. Electronic absorption spectra of $[\mathbf{1}]^{2+}$ (black) $[\mathbf{2}]^{2+}$ (red), $[\mathbf{3}]^{2+}$ (green), *trans*-$[\mathbf{4}]^{2+}$ (blue), and $[\mathbf{5}]^{2+}$ (cyan) measured in CH_3CN at room temperature.

Catalytic Tafel plots. For the catalysts employed in this study, which do not show ideal S-shaped catalytic waves, we used foot-of-the wave analysis (FOWA)[1] to derive intrinsic rates for [**3**]$^{2+}$ (*cis* & *trans* isomers) and *trans*-[**4**]$^{2+}$ during electrocatalytic CO_2 reduction at the corresponding first reduction potential for each complex. By applying equation (1) and plotting i/i_p vs $\{1+\exp[(F/RT)(E-E^0_{cat})]\}^{-1}$, we obtained the FOWA relationship, where the slope of the linear fit of this plot is equal to $2.24n\{(RT/Fvn_p^3)(k_{cat})[CO_2]\}^{1/2}$. Here, i is the catalytic current, i_p is the non-catalytic current in the absence of substrate (CO_2), R is the universal gas constant, T is the temperature, n is the number of electrons transferred from the electrode to the active catalyst (n = 2), n_p is the number of electrons transferred in the reversible non-catalytic reaction under inert atmosphere (n_p = 1), F is Faraday's constant, v is the scan rate, $C^o_{CO_2}$ is the concentration of CO_2 ($C^o_{CO_2}$ = 0.28 M in CH_3CN),[2] and k is the intrinsic rate constant, which can be written as a pseudo-first order rate constant $k_{cat} = kC^o_{CO_2}$. In all cases catalysis take place near to the first reduction potential of [**3**]$^{2+}$ and *trans*-[**4**]$^{2+}$, where E^o_{cat} is the standard reduction potential of the catalyst under inert atmosphere. With the catalytic rate constant in hand, Tafel plots were constructed by application of equation (2),[1b, 3] where overpotential, η, is plotted against log(TOF). The standard potential of the CO_2/CO couple in CH_3CN was taken as $E^o_{CO_2/CO}$ = −1.28 V vs. $Fc^{+/0}$ as derived by Savéant and co-workers[4] and converted to $Fc^{+/0}$ using a reported value.[5] The catalytic Tafel behavior for $[Ru^{II}(tpy)(bpy)(S)]^{2+}$ (S = solvent) was derived by application of equation (2) with k_{cat} = 7.6 s^{-1} obtained from previous reports.[6]

$$\frac{i}{i_p} = \frac{2.24n\sqrt{\frac{RT}{Fvn_p{}^3}}\sqrt{kC^o_{CO_2}}}{1 + exp\left[\frac{F}{RT}(E - E^o_{cat})\right]} \qquad (1)$$

$$TOF = \frac{k_{cat}}{1 + exp\left[\frac{F}{RT}\left(E^o_{CO_2/CO} - E^o_{cat} - \eta\right)\right]} \qquad (2)$$

References

[1] a) C. Costentin, M. Robert, J.-M. Saveant, *Chem. Soc. Rev.* **2013**, *42*, 2423-2436; b) C. Costentin, S. Drouet, M. Robert, J.-M. Savéant, *J. Am. Chem. Soc.* **2012**, *134*, 11235-11242; c) C. Costentin, J.-M. Savéant, *ChemElectroChem* **2014**, *1*, 1226-1236.

[2] A. Gennaro, A. A. Isse, E. Vianello, *J. Electroanal. Chem.* **1990**, *289*, 203-215.

[3] a) C. Costentin, G. Passard, J.-M. Savéant, *J. Am. Chem. Soc.* **2015**, *137*, 5461-5467; b) E. S. Rountree, B. D. McCarthy, T. T. Eisenhart, J. L. Dempsey, *Inorg. Chem.* **2014**, *53*, 9983-10002.

[4] C. Costentin, S. Drouet, M. Robert, J.-M. Savéant, *Science* **2012**, *338*, 90-94.

[5] V. V. Pavlishchuk, A. W. Addison, *Inorg. Chim. Acta* **2000**, *298*, 97-102.

[6] a) C. Costentin, G. Passard, M. Robert, J.-M. Savéant, *Proc. Natl. Acad. Sci. U. S. A.* **2014**, *111*, 14990-14994; b) Z. Chen, C. Chen, D. R. Weinberg, P. Kang, J. J. Concepcion, D. P. Harrison, M. S. Brookhart, T. J. Meyer, *Chem. Commun.* **2011**, *47*, 12607-12609.